The Gálvez-Davison Index for Tropical Convection

JOSE M. GALVEZ

Systems Research Group, College Park, Maryland

5830 University Research Court, Suite 4128, College Park, MD, 20740

jose.galvez@noaa.gov

MICHEL DAVISON

NOAA/NWS/NCEP Weather Prediction Center, College Park, Maryland

5830 University Research Court, Suite 4346, College Park, MD, 20740

michel.davison@noaa.gov

The Gálvez-Davison Index for Tropical Convection

José Manuel Gálvez (SRG/NOAA) and Michel Davison (NOAA)

ABSTRACT

The Gálvez-Davison Index (GDI) is developed to improve the prediction of tropical convection, due to the limited skill of traditional stability indices when used in the tropics, particularly in the Caribbean. The GDI considers thermodynamic properties of the low and mid troposphere. It is computed from temperatures and mixing ratios available at 500, 700, 850 and 950 hPa. It can thus be easily obtained from radiosonde data, gridded analyses, and numerical model output. The GDI considers three physical processes that modulate tropical convection: (1) the simultaneous availability of heat and moisture in the mid and low troposphere, (2) the stabilizing/destabilizing effects of a mid-level ridges/troughs, and (3) the entrainment of dry air and stabilization associated with trade-wind-type inversions.

A simple inter-comparison exercise over the Tropical and Subtropical Americas shows the GDI frequently outperforming traditional stability indices in the detection of varied convective regimes. It performs best in trade-wind regime climates and regions downwind, such as the northern Caribbean-Mexico and eastern Brazil. Inter-comparison results using a 2°×2° grid suggest that, in these regions, the GDI alone shares as much as ~50% and ~70% of the variance with brightness temperature and outgoing long wave radiation.

1. Introduction

The skill of numerical model forecasts of tropical convection tends to be poor. Weather forecasters thus need to rely on quantities such as stability indices to improve the accuracy of their predictions. Several traditional indices exist, but their skill decreases when used to forecast tropical convection. This indicates the need of an index specifically designed for this purpose.

The occurrence of convection relates to the thermodynamical properties of air columns and to dynamical processes. The role of thermodynamics is particularly important in the tropics, where dynamical processes are usually weak. The connection between convection and column thermodynamics has led to the development of stability indices since the 1940s. A list of commonly used ones is summarized in Table 1. Stability indices are defined as quantities designed to provide prompt but comprehensive evaluations of the static stability of air columns, and to be readily computed from sounding data (Glickman, 2000). Weather forecasters find them useful as they reduce the time required to produce a forecast of convection. There are other quantities considered as effective parameters for forecasting convection, such as the Convective Available Potential Energy (CAPE), and the Convective Inhibition (CIN) (Glickman, 2000). Other indices that relate to convection exist, but their main focus relies on other aspects of it such as severity, e. g. the SWEAT index (Miller 1972). A comprehensive list and description of indices used for thunderstorm forecasting can be found in Harklander and Van Delden (2003).

TABLE 1. Traditional Stability Indices actively used to forecast moist convection.

Index	Reference	Summary
Showalter	Showalter (1947)	Estimates convective instability by comparing the difference between the 500 hPa ambient temperature and that of a parcel rising from 850 hPa following the dry adiabat until saturated, and then the moist adiabat.
K	George (1960)	The K was developed to forecast air mass thunderstorms. It considers an 850-500hPa lapse rate term and an 850-700 hPa moisture term. The consideration of 700 hPa moisture adds skill in tropical environments. Limitations are performance over elevated terrain and spatial homogeneity in the deep tropics.
Lifted	Galway (1966)	Similar to the Showalter index, but the parcel is lifted from the boundary-layer top instead of 850 hPa. Although methods for the determination of this level vary, it is often determined using the warmest diurnal temperature and the mean mixing ratio at 2m, predicted if necessary. This height often falls within the lowest 900m of the profile. Lifted index values tend to be lower than Showalter index values.
Total Totals	Miller (1967)	It is based upon an 850-500hPa lapse rate term and upon a cross moisture-temperature term. The latter is largely sensitive to 850 hPa moisture. It was designed for applications in the United States (Peppler and Lamb, 1989).

The limitations of the traditional stability indices when applied to tropical environments are addressed in Atkinson (1971) and Ramage (1995). These limitations arise from differences in the physical processes that modulate tropical versus extra tropical convection (Schultz, 1989; Jacovides and Yonetani, 1990; Huntrieser et al., 1997; Harklander and Van Delden, 2003). An example is shown in Figure 1, which illustrates how three traditional stability indices and CAPE struggle to capture the regions where deep tropical convection developed. Deep convection is here interpreted as persistent cold cloud tops (central upper panel in Figure 1) which can be recognized as low brightness temperatures BT persisting over the averaging period. Scalloped outlines encircle regions of BT averages lower than -10°C, which generally relate to persistent moderate-to-deep convection, and are overlaid on index data for inter-comparison (surrounding panels). The discrepancies shown in Figure 1 represent a repeatedly encountered outcome when traditional stability indices are used in tropical environments.

Figure 1 also illustrates the relative skill of the K index – developed to forecast air mass thunderstorms (George, 1960) – when compared to the performance of the Total Totals Index TTI, the Lifted Index LI and the CAPE. This relative skill arises from the consideration of 700 hPa moisture (Caesar, 2005), a quantity closely related to buoyancy and dry air entrainment in the tropical mid-troposphere. Still, the K index exhibits some limitations in tropical environments. These include low variability in shallow convective regimes, particularly in equatorial latitudes; and the disregard of thermodynamic properties below 850 hPa, which are important to determine the stability and moisture availability in the boundary-layer.

The need of a skillful index for the prediction of tropical convection motivated the Weather Prediction Center (WPC) International Desks to develop the Gálvez-Davison Index (GDI). The GDI emphasizes processes that modulate tropical convection, particularly trade wind

convection. As will be later shown, validation results and user comments are encouraging. The manuscript is organized in six sections. Section 2 discusses background concepts relevant to the calculation of the GDI. Section 3 presents the rationale and the calculation algorithm. Section 4 shows the results of a simple inter-comparison exercise. Section 5 elaborates on the applicability of the GDI. Section 6 closes with concluding remarks and recommendations.

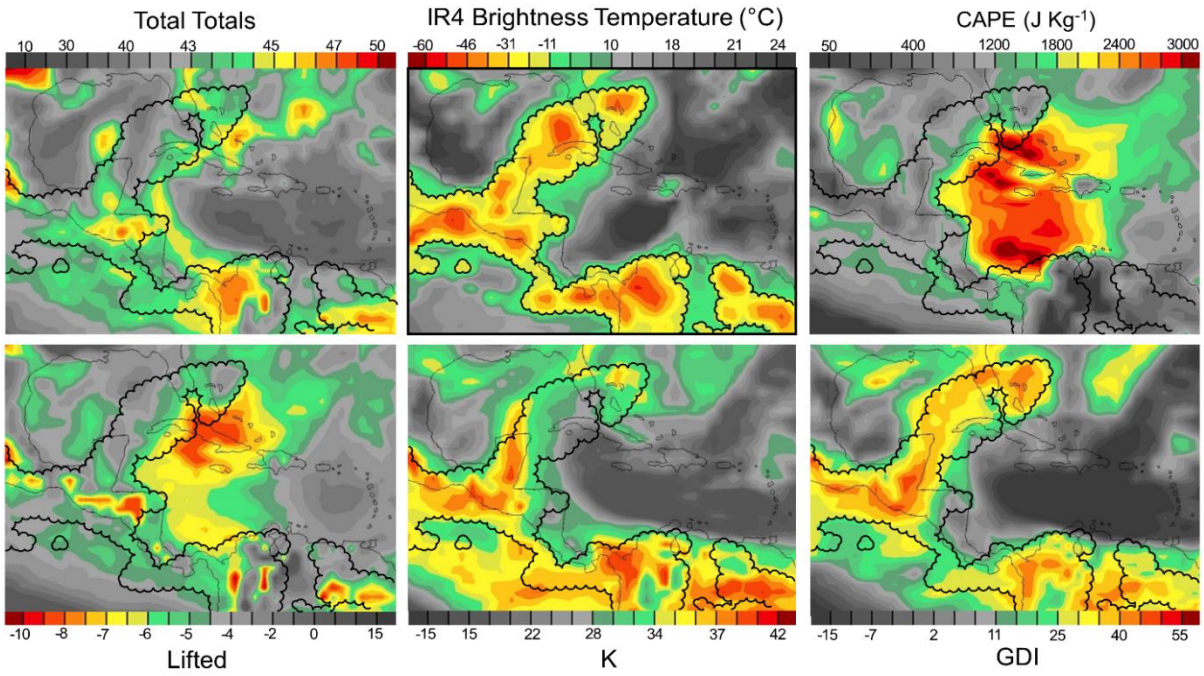

FIG. 1. Intercomparison of GOES IR4-derived BT (top center) against CAPE (top right) and four stability indices (remaining panels) computed from GFS F00-F12 data. All fields are averages over the 16 August 2013 00-12 UTC period. The curly outlines encircle regions where BT averages were colder than -10°C.

2. Background

a. Processes that modulate tropical convection

The balance of physical processes involved in the modulation of convection differs between the tropics and the extra tropics (Atkinson, 1971; Ramage, 1995). While in the extra tropics the role of stability is substantial, in the tropics, that of moisture gains relative importance. Tropical convection is generally sensitive to dry air entrainment due to the frequent absence of strong dynamical forcing mechanisms. Moist layers are associated with decreased potential instability due to both the temperature and dew point profiles approaching the moist adiabat. Although this implies some stabilization, moist tropical environments are more suitable for convective development and maintenance than less stable but drier ones. Convection in such moist tropical environments is often triggered by convective downdrafts and resulting near–surface convergence and lift (Grabowski and Moncrieff, 2004; Tompkins, 2001; John Knaff, personal communication, 2015). Surface heat fluxes and infrared radiation, are generally tied to the local geography and convection itself (Randall and Huffman, 1980; Grabowski and Moncrieff, 2004), and also play a role.

To forecast tropical convection, it is thus important to determine the potential for moistening of the tropical low and mid troposphere. Moistening in the tropics can occur from large scale advection, but is primarily produced by foregoing convection (Randall and Huffman, 1980; Grabowski and Moncrieff, 2004). This is the Moisture-Convection feedback mechanism (addressed in Section 2), which suggests that foregoing convection in upstream locations could be used as a predictor for tropical convection. This is a key concept behind the GDI formulation.

Moisture content alone is not sufficient to accurately evaluate the potential for convection in the tropical atmosphere. Other processes such as the trade wind inversion (TWI) and mid-level cold/warm core systems strongly modulate thermal and moisture profiles. The TWI (Riehl, 1954) is an extensive subsidence inversion that forms in the descending branches of the Hadley circulation (Raymond 2000b), and dominates vast areas of the tropics. It is typically characterized by a mild decrease in the lapse rate – sometimes by an actual increase of temperature with height – and often by a sharp decrease in moisture from base to top. These features largely control cloud growth through enhanced negative buoyancy and dry air entrainment. Strong and/or lowered inversions limit vertical development, but weak and/or elevated inversions can allow some cloud growth. If deep convection manages to develop through a weak or elevated inversion, it releases water vapor into the free troposphere leading to an 'unexpected' moistening. The moistening constructs an environment favorable for the development of new convective cells, ultimately establishing the Moisture-Convection feedback mechanism described by Grabowski and Moncrieff (2004), and a fair-to-stormy weather transition. Considering the structure of the TWI is thus essential for an accurate prediction of tropical convection. Figure 2 illustrates this concept.

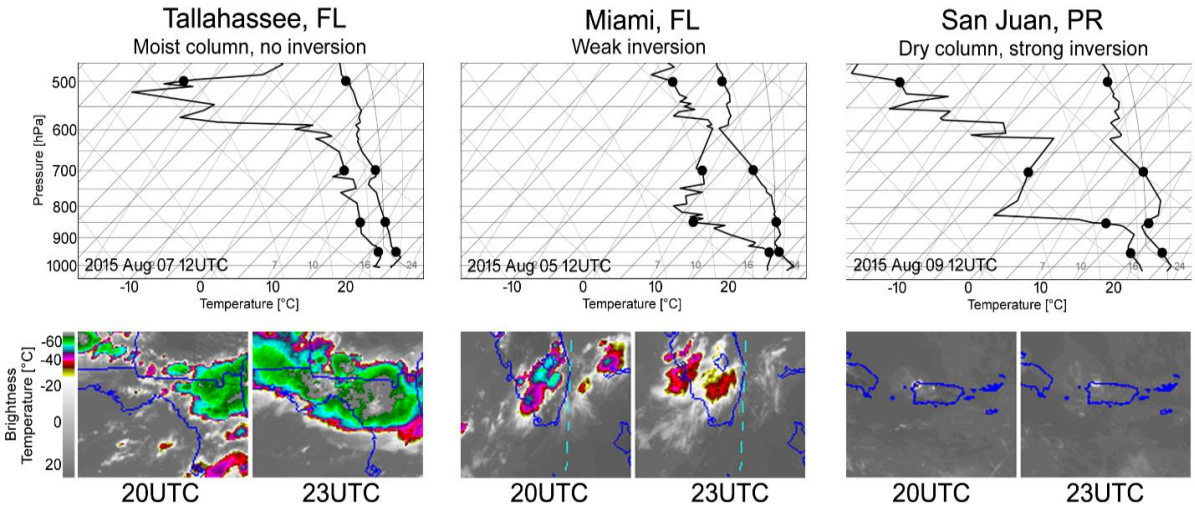

FIG. 2. 12UTC soundings (top) and corresponding GOES IR4-derived BT near 20 UTC and 23 UTC (bottom) for three locations: Tallahassee, FL (left); Miami, FL (center), and San Juan, Puerto Rico (right). The figure illustrates the evolution of afternoon convection near/downstream of each station in association with the morning sounding. The GDI calculation points are included in the soundings for later reference. Soundings are courtesy of the University of Wyoming (http://weather.uwyo.edu/upperair/sounding.html, 2015) and satellite images courtesy of CIRA (http://rammb.cira.colostate.edu/ramsdis/online/rmtc.asp, 2015).

Figure 2 compares three rainy season morning soundings with different TWI features. The resulting afternoon convective regimes are described using GOES IR4-derived BTs. The Tallahassee, Florida sounding (left) shows no inversion and a very moist column from the surface through 600hPa. This favored the development of widespread afternoon thunderstorms that continued intensifying from the middle (20 UTC) through the late afternoon (23 UTC). The San Juan, Puerto Rico sounding (right) contrasts with the Tallahassee sounding as it shows a strong TWI near 850 hPa accompanied by a thick dry layer aloft. This limited development to isolated rain showers. An isolated thunderstorm developed as well, but weakened rapidly by the entrainment of dry air in the free troposphere. The Miami, Florida sounding falls in between. It shows a very weak TWI with moist layers aloft, especially between 650 and 550hPa. This allowed the development of scattered thunderstorms in the early afternoon, yet, the storms were already weakening by 23 UTC. The structure of the TWI is variable in space and time, and does play an important role in the variability of trade wind convection.

Mid-level circulations are also important for the development of tropical convection. Dynamics aside, mid troughs/ridges are associated with cool/warm cores that enhance/decrease the stability of the underlying troposphere. The Tropical Upper Tropospheric Trough (TUTT) (Sadler, 1967) is a common feature in trade wind climates, especially during the rainy season, and has a role in trade wind convection. When a TUTT expands from the upper into the mid troposphere, its cold core generates sufficient destabilization in underlying layers to enhance convective growth. Although not relevant to the calculation of stability, mid-level troughs/ridges also exert dynamical effects on the underlying air mass as they frequently associate with ascent/subsidence. This is reflected to some extent whenever mid tropospheric temperatures are considered in the computation of stability.

b. Equivalent potential temperature and tropical convection

The equivalent potential temperature (EPT) is a useful quantity to assess moisture content, as well as thermal properties of the air column. EPT is the final temperature that an air parcel would attain if lifted dry adiabatically to its lifting condensation level, then moist adiabatically until all water vapor, and finally brought down dry adiabatically to 1000 hPa (Holton, 1972; Bolton, 1980; Bryan, 2008). EPT thus relates to column moisture and to the potential release of latent heat. It therefore provides information about the potential for additional moistening of the column. The WPC International Desks have long relied on EPT profiles to determine the potential for convection in the Tropical Americas, especially the Caribbean. EPT profiles not only depict warm moist columns but do capture the signature of TWI. These appear as sharp decreases of EPT with height due to the overwhelming effects of the decrease in moisture over the subtle increase in temperature across the inversion. Figure 3 illustrates this.

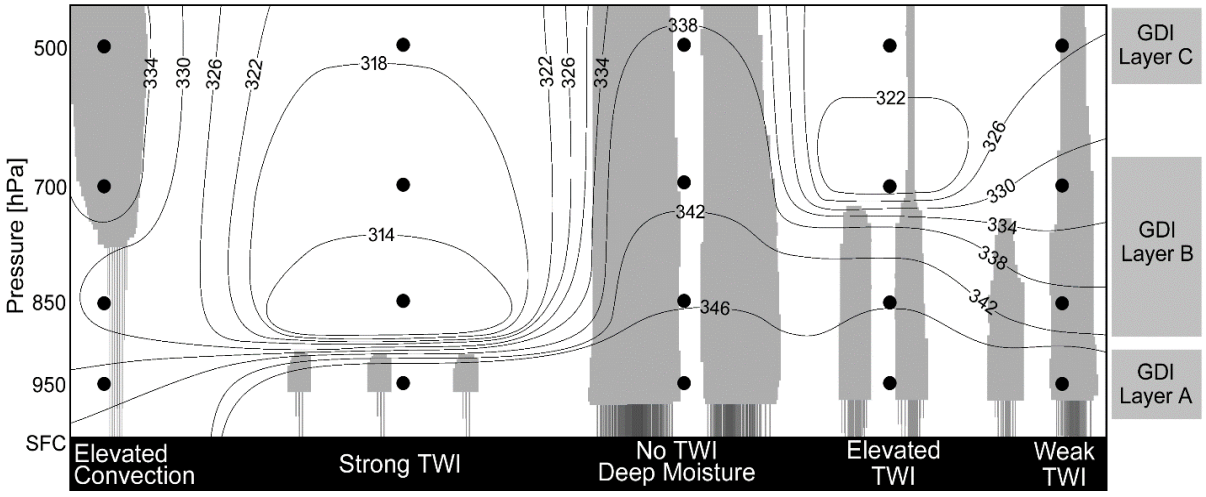

FIG. 3. Schematic representation of an EPT cross section characteristic of trade wind regimes (black contours in K). Associated convection and precipitation are sketched in grey. Five different convective regimes are shown, for which GDI calculation points are indicated with black circles. The three layers used for the formulation of the GDI are included to the right.

Figure 3 is a schematic representation of the signature of five commonly encountered trade wind convection regimes on an EPT cross section. The most favorable environment for deep convection – and potentially heavy rainfall – is shown in the center, and is characterized by large EPT values that decrease gently with height. Conversely, the potential for deep convection minimizes under strong TWI, especially when they occur at heights below 850 hPa. Their signature on EPT profiles consists of a sharp decrease with height across the inversion. Lowered and/or strong TWI confine activity to light rain showers, yet, their intensity is still sensitive to moisture content in the marine layer. This is relevant to the use of 950 hPa instead of 925 hPa data for the GDI formulation, as will be detailed in section 3.

Figure 3 also illustrates the signature of three convective regimes that fall in between. An elevated TWI, identified as a sharp EPT decrease in the mid troposphere, often allows sufficient development for convection to produce moderate rains. A few cells can penetrate the inversion and evolve into thunderstorms, but they are often isolated and short lived due to dry air entrainment aloft. A weak TWI can also favor thunderstorm development but convection life span and rainfall amounts rarely exceed those that develop when the TWI is absent. Elevated convection also occurs in the tropics, and reflects as an EPT maxima near/above 700 hPa accompanied by a relatively homogeneous profile underneath. Electrification is possible, and under favorable conditions, rainfall rates can be comparable to that generated under weak and elevated TWI.

The close relationship between the vertical distribution of EPT and trade wind convection types motivated the use of EPT as part of the GDI calculation algorithm (Section 3). Calculating EPT is, however, non-trivial. Several approaches exist, as detailed in the comprehensive summary provided by Davies-Jones (2009). EPT discrepancies produced by these different formulas are negligible in the context of weather forecasting. This motivated

the selection of a simplified expression. The following formula, simplified by Bolton (1980) after Betts and Dugan (1973), was selected:

$$\theta_E = \theta \exp\left(\frac{L_o r}{C_{pd} T_{LCL}}\right) \tag{2.1}$$

where L_o=2.69 × 10^6 J kg^{-1} is the latent heat of vaporization, C_{pd}=1005.7 J kg^{-1} K^{-1} is the specific heat of dry air at constant pressure, θ is the potential temperature [K], r the mixing ratio [kg kg^{-1}] and T_{LCL} the temperature at the lifted condensation level LCL [K]. The complex calculation in this formulation is the determination of T_{LCL}. While developing the GDI, testing revealed that replacing T_{LCL} with 850 hPa temperatures [K] produced very small differences on the final GDI values. This greatly simplifies the calculations and leads to the following expression for the calculation of EPT proxies to be used in the GDI formulation:

$$\theta_{E\_GDI} = \theta \exp\left(\frac{L_o r}{C_{pd} T_{850}}\right) \tag{2.2}$$

3. Algorithm for the calculation of the Gálvez-Davison Index.

The GDI consists of the algebraic sum of three dimensionless sub-indices and a terrain correction factor. Each of these indices describes a tropospheric feature that is relevant to the development of tropical convection. The GDI calculation expression is:

$$GDI = CBI + MWI + II + TC \tag{3.1}$$

where CBI is a Column Buoyancy Index, MWI is a Mid-Tropospheric Warming Index, II is an Inversion Index, and TC is the optional terrain correction. The GDI was intentionally developed to produce values similar to those of the K, for which a few empirical adjustment constants were determined ad hoc.

Input variables consist of temperatures and mixing ratios available at 950, 850, 700 and 500 hPa. The 950 hPa level was chosen instead of the 925hPa mandatory level to ensure the consideration of boundary-layer information. This is particularly important in environments with lowered TWIs, which sometimes lie below the 850hPa level. These four levels are used to define the three layers shown in Figure 3. Layer A represents thermodynamic conditions in the boundary-layer. Layer B captures the variability associated with the TWI using a simple average of 850 and 700 hPa data. Layer C represents the mid troposphere by considering 500 hPa data.

Potential temperatures θ and mixing ratios r are first calculated for each layer via:

$$\theta_A = \theta_{950} = T_{950}(1000/950)^{2/7} \tag{3.2}$$

$$r_A = r_{950} \tag{3.3}$$

$$\theta_B = 0.5(\theta_{850}+\theta_{700}) = 0.5[T_{850}(1000/850)^{2/7}+T_{700}(1000/700)^{2/7}] \quad (3.4)$$

$$r_B = 0.5(r_{850}+r_{700}) \quad (3.5)$$

$$\theta_C = \theta_{500} = T_{500}(1000/500)^{2/7} \quad (3.6)$$

$$r_C = r_{500} \quad (3.7)$$

EPT proxies are then calculated by applying equation 2.2 to each layer:

$$EPTP_A = \theta_A e^{(\frac{L_o r_A}{C_{pd} T_{850}})} \quad (3.8)$$

$$EPTP_B = \theta_B e^{(\frac{L_o r_B}{C_{pd} T_{850}})} + \propto \quad (3.9)$$

$$EPTP_C = \theta_C e^{(\frac{L_o r_C}{C_{pd} T_{850}})} + \propto \quad (3.10)$$

where $\propto = -10$ [K] is an empirical adjustment constant designed to limit excessive GDI values in regions with plentiful moisture at and above 850 hPa. These EPT proxies are then used for the calculation of the three GDI sub-indices as detailed in the following.

a. Column Buoyancy Index

The CBI describes the availability of heat and moisture in the column. It is the only sub-index of the GDI that produces positive values, thus can be considered as the enhancement sub-index. The CBI becomes largest when a warm and moist mid troposphere (layer C) is reinforced by warm and moist conditions near the surface (layer A). Large values suggest the presence of a deep moist layer that has the potential of hosting deep convection and potentially heavy rainfall. To compute the CBI, EPT factors are first calculated for the mid (ME) and low (LE) troposphere, and are subsequently used to calculate the CBI with a conditional expression:

$$ME = EPTP_C - \beta \quad (3.11)$$

$$LE = EPTP_A - \beta \quad (3.12)$$

$$CBI = \{ \begin{matrix} \gamma \times LE \times ME & , LE > 0 \\ 0 & , LE \leq 0 \end{matrix} \} \quad (3.13)$$

where $\beta = 303$K is an empirical constant designed to set a lower boundary for the availability of heat and moisture in the boundary-layer. This disregards air masses that are too dry and/or cool, which sets the CBI to zero. The constant $\gamma = 6.5\times10^{-2}$ [K^{-1}] is an empirical scaling quantity used to attain dimensionless values in ranges similar to those of the K index.

b. Mid tropospheric Warming/Stabilization Index

The MWI accounts for stabilization/destabilization in association with warm ridges/cool troughs in the mid troposphere. It is an inhibition factor, meaning that it produces only negative

values or zero. Negative values occur when 500 hPa temperatures exceed the threshold $\tau = 263.15$K or -10°C. Warmer 500hPa temperatures above this threshold relate to stronger inhibition. The MWI is calculated via

$$MWI = \{ \begin{matrix} \mu\times(T_{500} - \tau) & ,T_{500} - \tau > 0 \\ 0 & ,T_{500} - \tau \leq 0 \end{matrix} \} \quad (3.14)$$

where $\mu = -7$ [K^{-1}] is an empirical scaling constant determined ad hoc to sets MWI values negative, and to control the relative weight of the MWI on the GDI formula (equation 3.1).

c. Inversion Index

The II is also an inhibition factor designed to capture the effects of TWI. It considers two processes that inhibit trade wind convection: stability across the inversion and dry air entrainment once convective cells penetrate it. It consists on the algebraic sum of two dimensionless factors: a stability factor S and a drying factor D. The following conditional expression is used to set positive values to zero:

$$II = \{ \begin{matrix} 0 & ,S + D > 0 \\ \sigma\times(S + D) & ,S + D \leq 0 \end{matrix} \} \quad (3.15)$$

where $\sigma = 1.5$ [K^{-1}] is an empirical scaling constant determined ad hoc to control the weight of TWI effects on the GDI formulation (equation 3.1). D is a lapse rate term, and is calculated via a simple difference of 950 and 700 hPa temperatures [K] via:

$$S = T_{950} - T_{700} \quad (3.16)$$

The lower the difference, the stronger the stabilization due to an increase in negative buoyancy. D is calculated using the difference of EPT factors from layers A and B:

$$D = EPTP_B - EPTP_A \quad (3.17)$$

and accounts for the effects of dry air entrainment across the inversion. The larger the decrease of EPT with height, the more negative D becomes, meaning more dry air entrainment and inhibition of convective development.

d. Terrain correction

Improved visualization of predictor fields matters in weather forecasting practices, as this optimizes the time required by the forecaster to draw conclusions and produce a forecast. Strictly speaking, the GDI should be only applicable in places located below 950 hPa. Numerical model data, however, is commonly interpolated to fill in layers that, in reality, lie under the model surface. These data do contain information that can be used productively to adjust high GDI values over high terrain into more realistic ones. Accordingly, a dimensionless terrain-correction factor TC is calculated with surface pressure P_{SFC} [hPa] for improved visualization/interpretation over high terrain:

$$TC = P_3 - \frac{P_2}{P_{SFC} - P_1} \quad (3.18)$$

where P_1=500 [hPa], P_2=9000 [hPa] and P_3=18 are all empirical constants. As will be shown, the validation exercise and user comments indicate that the correction still allows for high GDI-cold cloud top correlations in mountainous regions. A relevant example are the Mexican highlands, where the GDI shares more than 50% of the variance with BT when data is compared using a 2° horizontal resolution.

4. Inter-comparison exercise.

a. Method

A short inter-comparison exercise was used as a first approach to evaluate the skill of the GDI in the tropical and subtropical Americas. Validation was carried out using data from the 2013-14 rainy seasons. Details on the method are provided in Tables 2 and 3. The first exercise compared GFS-derived GDI values against GOES IR4 BTs over Mexico, Central America, the Caribbean and the southeastern United States. The exercise was later extended to include South America (Table 3). One difference was the consideration of Outgoing Long Wave Radiation OLR instead of BT data due to practical reasons regarding data accessibility and computational resources. Yet, both BT and OLR describe the general structure and depth of tropical convection. Some contamination by cirrus clouds is unavoidable, especially in the vicinity of mesoscale convective systems and ascending subtropical upper jets. The latter are, however, rarely present during the rainy seasons.

As a simple means for index performance evaluation, the dimensionless determination coefficient r^2 was used:

$$r^2 = \frac{n\sum xy - (\sum x)(\sum y)}{\sqrt{n(\sum x^2) - (\sum x)^2}\sqrt{n(\sum y^2) - (\sum y)^2}} \quad (4.1)$$

where n is the sample size, x corresponds to BT [K] for North America and OLR [W m^{-2}] for South America; and y corresponds to index values. The r^2 quantifies the fraction of the variance shared by the quantities compared.

To assess the performance of the GDI relative to that of traditional stability indices, the LI, TTI, K indices and CAPE were also computed from GFS output as indicated in Tables 2 and 3. The data were intercompared at two different horizontal resolutions: 1° and 2°, and a comparison of the effects of resolution are illustrated in Figure 4. It is natural to expect a significant increase in index skill when data is compared at coarser resolutions, as numerical models sometimes capture features but resolve them displaced by tens or even hundreds of kilometers. This is especially true in the case of tropical convection as it organizes into complex but discrete mesoscale structures. In Figure 4, r^2 of BT versus the GDI (top) and

versus the K (bottom) illustrates the increase of index skill with decreasing horizontal resolution. With this in mind, intercomparison fields will be hereafter presented using resolutions of 2° for all quantities.

TABLE 2. Data used for the validation of the GDI over tropical North America and the Caribbean.

Data	Averaging Method	Original data source
Brightness Temperatures	12-hr averages (00-12Z) computed daily during 01 July – 31 October 2013.	30-minute GOES-13 IR4 data courtesy of RAMSDIS*.
Index values	12-hr averages (00-12Z) computed daily during 01 Jul – 31 October 2013.	6-hour GFS 00Z analyses and forecasts (00-F12) from NCEP§.

* Available online at: http://rammb.cira.colostate.edu/ramsdis/online/rmtc.asp
§ Available online at: ftp://tgftp.nws.noaa.gov/SL.us008001/ST.opnl/

TABLE 3. Data used for the validation of the GDI over tropical South America.

Data	Averaging Method	Original data source
Outgoing Long Wave Radiation	24-hr averages (00-24Z) computed daily during 01 October 2013 – 28 February 2014.	Daily OLR data courtesy of NCEP* (Liebmann and Smith, 1996).
Index values	12-hr averages (00-12Z) computed daily during 01 Jul – 31 October 2013.	6-hour GFS 00Z analyses and forecasts (00-F12) from NCEP§.

* Available online at: http://rammb.cira.colostate.edu/ramsdis/online/rmtc.asp
§ Available online at: ftp://tgftp.nws.noaa.gov/SL.us008001/ST.opnl/

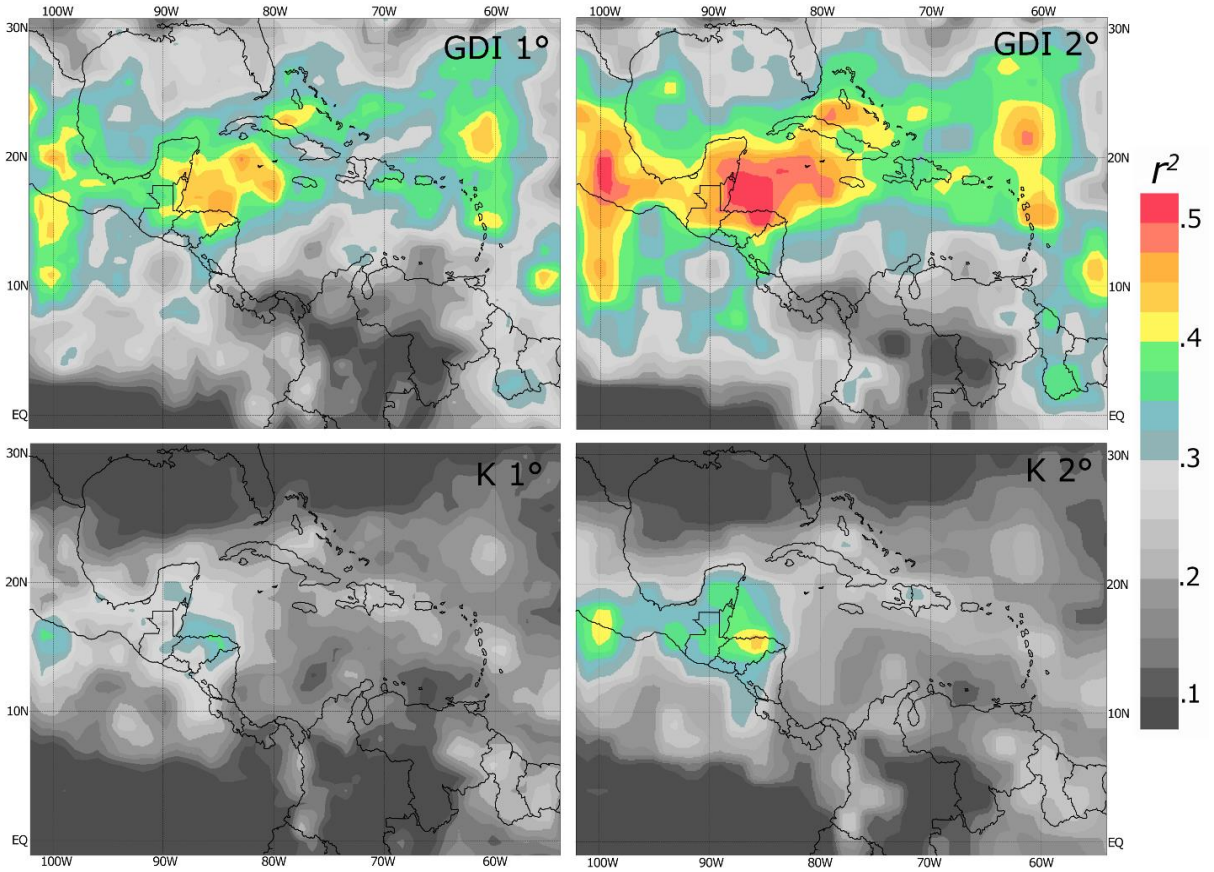

FIG. 4. Determination coefficient r^2 computed for BT-GDI (top) and BT-K (bottom) and at horizontal resolutions of 1° (left) versus 2° (right). The values were computed using daily 12-hr (00-12 UTC) averages for the 01 July – 31 October 2013 period.

One limitation of the exercise is the conditioning of index skill to that of the first 12 and 24 hours of the 00UTC GFS outputs (see Tables 2 and 3). During these periods, however, index-cold cloud r^2 values are reliable under the assumption that the model captured the tropospheric evolution reasonably well. This is generally true, which is documented in verification results prepared by the Global Climate and Weather Modeling Branch of the NCEP's Environmental Modeling Center (http://www.emc.ncep.noaa.gov/GFS/perf.php). Index skill intercomparison is however barely compromised given that index values are computed from the same data.

b. Discussion of the results

The results are encouraging as they show that the GDI outperforms most stability indices on the depiction of tropical convection. This is illustrated in Figure 5 for North/Central America and the Caribbean. Here, a comparison of r^2 calculated for the five stability indices/quantities tested shows that the largest index-cold cloud correlations for a given point are generally attained by the GDI. The largest GDI-cold cloud correlations occur along the 15°N-25°N belt that stretches from the central Caribbean/Nicaragua northward into most of Mexico and the Florida peninsula. This includes the Bahamas, Leeward Islands and the Greater Antilles, where the GDI was able to relate to more than 35% of BT variance. The skill is particularly remarkable in the Gulf of Honduras/Yucatan Peninsula and in central Mexico,

where the GDI relates to more than 45% of BT variances. The high correlations encountered in Mexico are particularly noteworthy given that most of the terrain lies above 950 hPa. This is an encouraging result as central Mexico is a largely populated region that includes Mexico City, an urban area that comprises near 20 million people.

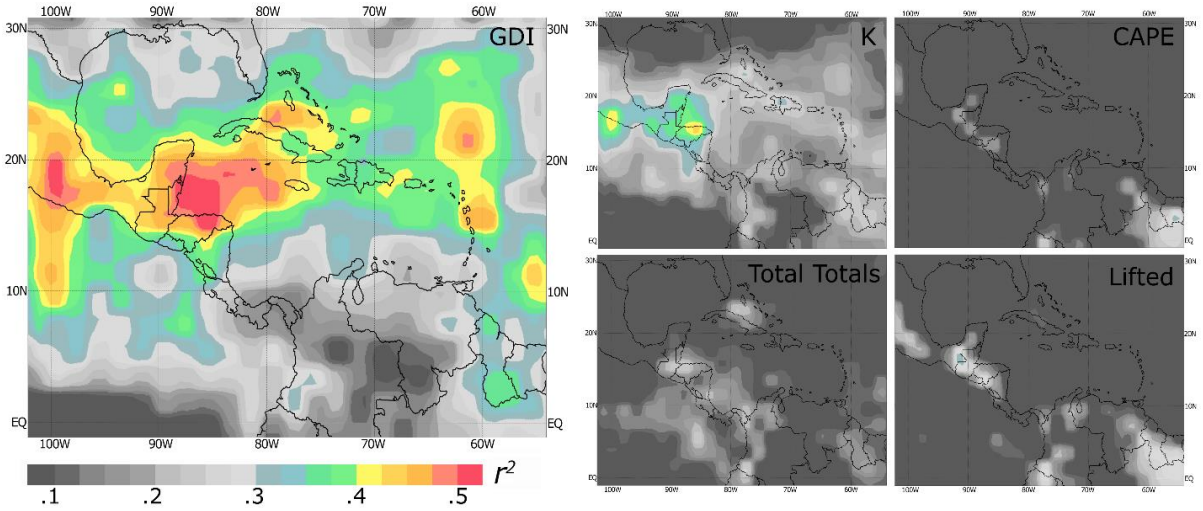

FIG. 5. Determination coefficient r^2 for BT against the GDI (left), K (top center), CAPE (top right), TTI (bottom center) and LI (bottom right), computed over tropical North America and the Caribbean using daily 12-hr averages (00-12 UTC) during the 01 July – 31 October 2013 period.

Index-BT r^2 were compared by simple differences, and are presented in Figure 6. The prevalence of yellows and reds shows how the GDI outperforms all indices across most of the domain. The increased skill over other indices is remarkable within the 15°N-30°N belt. This includes the Florida Peninsula and the Gulf of Mexico. Here, the GDI relates to an additional 15+% of BT variance than the K, and, in some instances an additional 30+% when compared against CAPE, and the Total Totals and Lifted indices. This indicates that, in these regions, the GDI appears to be the most skillful index for the forecasting of convection. Its skill decreases in areas close to the intertropical convergence zone ITCZ and Panamanian Low, generally located near/over Southern Central America/northwestern Colombia. This is related to the limited presence of TWI and cool mid-level troughs in the deep tropics during the peak of the rainy season.

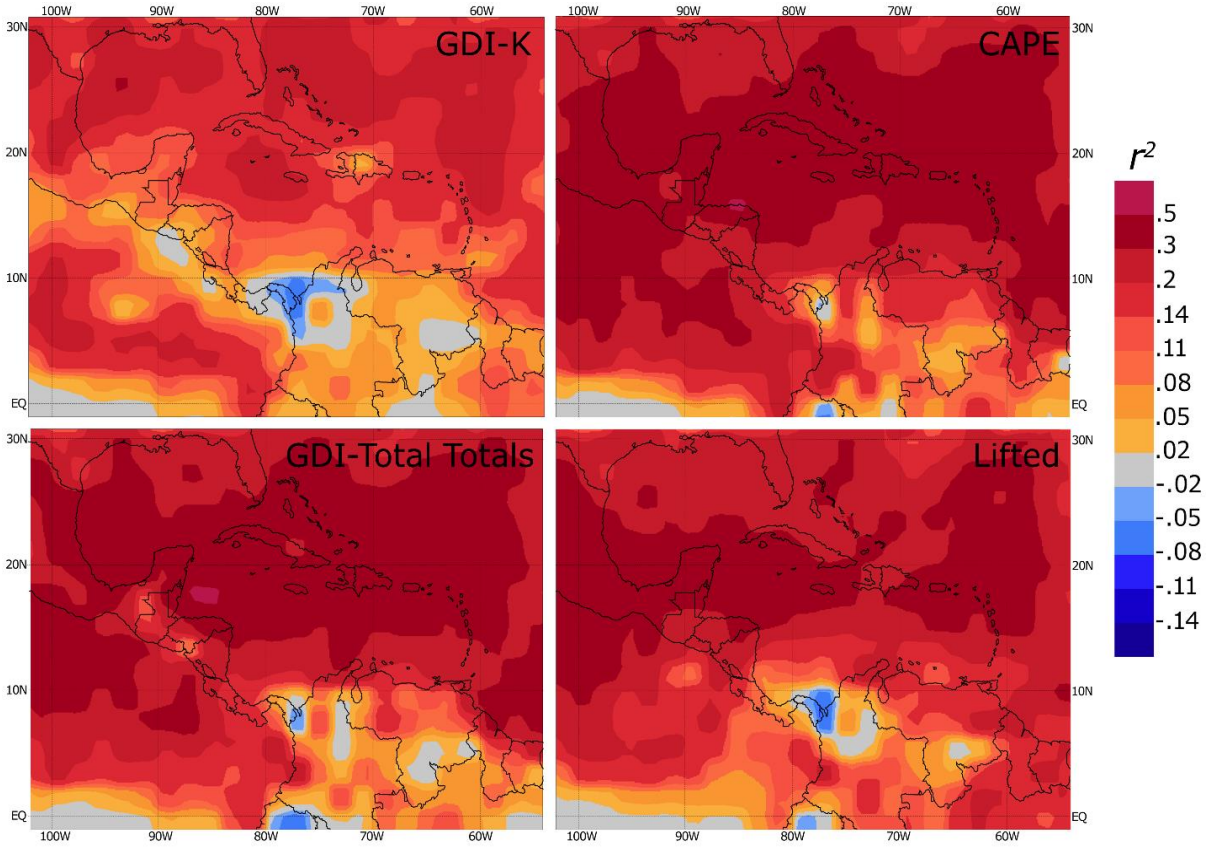

FIG. 6. Algebraic differences between the r^2 of BT-GDI minus those of (a) BT-K, (b) BT-LI and (c) BT-TTI, computed for tropical North America and the Caribbean using daily 12-hour averages (00-12 UTC) during the 01 July – 31 October 2013 period.

A similar analysis was conducted over South America and presented in Figures 7 and 8. Here, the GDI was also able to outperform the traditional stability indices and CAPE over most of the domain. The GDI was also able to relate to more than 45% of cold cloud variances over vast areas of eastern Brazil and Venezuela, all dominated by trade wind regimes. Surprisingly, the correlations found in some of these regions were larger than those found in Central America and the Caribbean, as r^2 exceeded 70% in parts of the states of Minas Gerais and Espirito Santo in southeastern Brazil. This is also encouraging, as densely populated areas such as Sao Paulo and Rio de Janeiro lie within this GDI-skill belt. These preliminary results, and intercomparison with other indices, place the GDI as the best index available for the forecasting of convection in Southeastern Brazil. This is similar to the results found in Florida and the Gulf of Mexico.

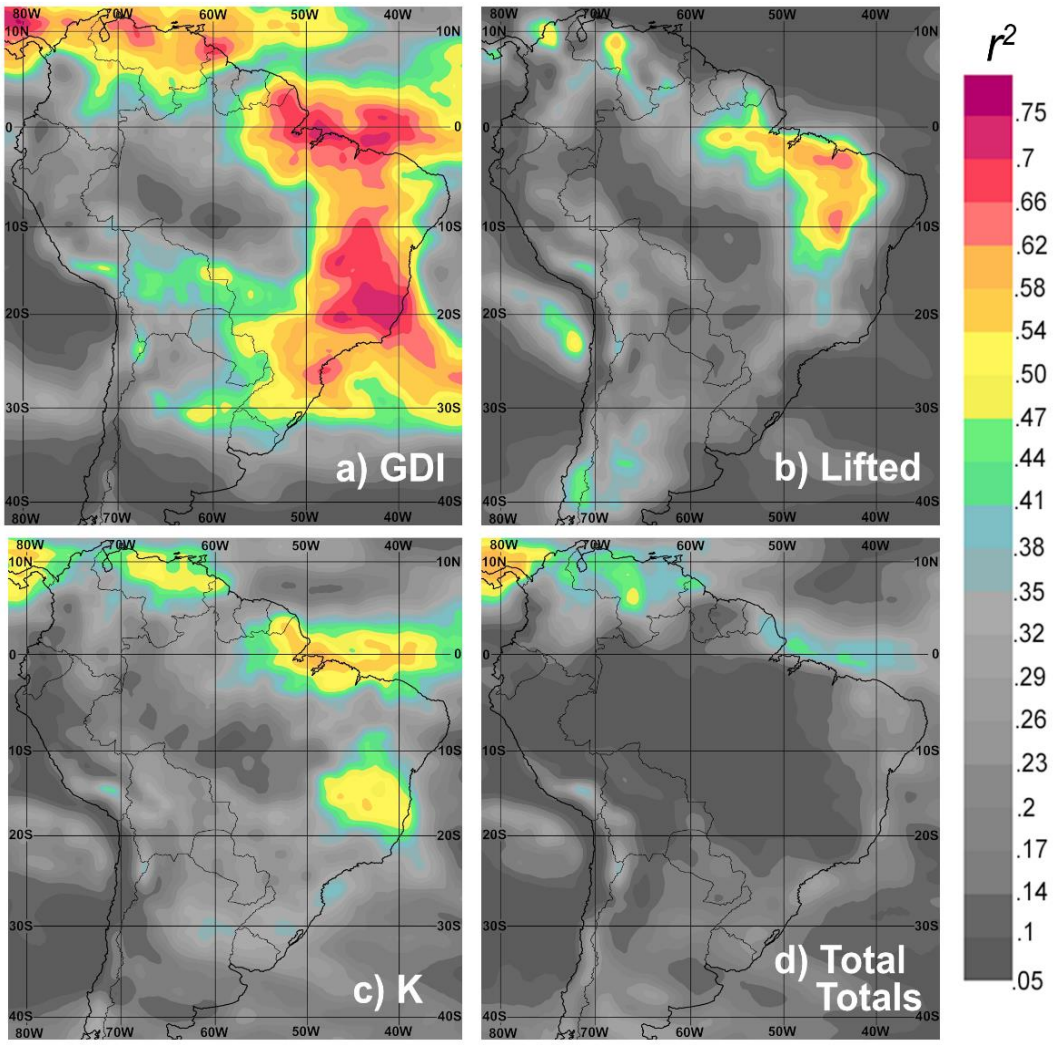

FIG. 7. Determination coefficient r^2 for BT against the (a) GDI, (b) LI, (c) K, and (d) TTI, computed for central and northern South America using daily 24-hr averages during the 01 October 2013 – 28 February 2014 period.

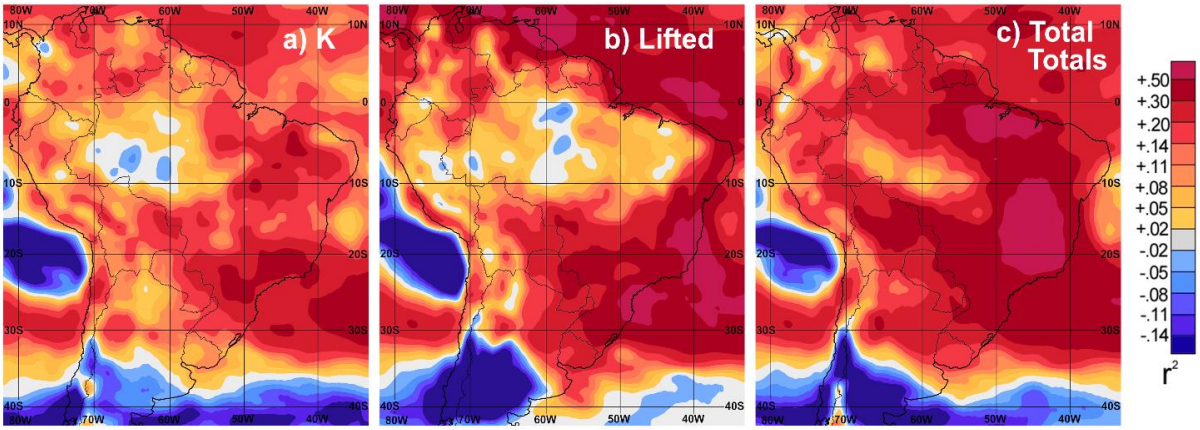

FIG. 8. Algebraic differences between r^2 of BT-GDI minus those of (a) K-BT, (b) LI-BT and (c) BT-TTI computed for central and northern South America using daily 24-hr averages during the 01 October 2013 – 28 February 2014 period.

An interesting result are the larger correlations found in northern Venezuela during their dry season (Figure 7) when compared against those attained during the rainy season (Figure 4). This indicates decreased GDI skill in persistent ITCZ and deep-tropical convection environments. This is an expected finding given the decreased variability in mid-level temperatures and TWI absence during the peak of the rainy season. This is also the case in the central and western Amazon basin (western Brazil, eastern Peru) during their rainy season. Here, air masses that arrive from the east have lost their trade-wind thermodynamic characteristics after interacting with most of Tropical South America.

Index skill intercomparison, presented in Figure 8, also shows encouraging results. As in North/Central America and the Caribbean, the GDI outperforms most indices across most of tropical and subtropical South America. This is particularly true in eastern Brazil, a region with a trade wind climate similar to that of the Caribbean. In eastern Brazil, the GDI relates to an additional 15-30% of the OLR variance than the K. The enhanced skill extends west into Paraguay/Bolivia and southern Peru, where the GDI relates to an additional 10-20% of the variance resolved by the K. The most remarkable skill improvement coincides with densely populated regions of southeastern Brazil across the states of Paraná, Sao Paulo, Minas Gerais, Rio de Janeiro and Espirito Santo where the GDI relates to 30+% of the OLR variance resolved by the K.

Figure 8 also shows how other indices, especially the Lifted and Total Totals outperform the GDI in extra tropical locations that stretch south of a line from Central Chile into extreme northern Patagonia/southern Buenos Aires province in Argentina. This is also an expected result due to the GDI dependence on deeper tropical/subtropical moisture. The GDI becomes occasionally useful in mid latitude western coasts such as central Chile. This occurs when robust atmospheric rivers/subtropical moisture connections establish and arrive into continental areas. GDI skill is also limited over the cold current stratocumulus regime off the coasts of northern Chile and southern Peru, which relates to differences in the thermal structure of this cold current versus trade wind regimes (i.e. cold current boundary-layers are much cooler than trade wind regime ones).

Validation results also indicate that the GDI can be used in extra tropical locations during the summer. In these environments, however, it is especially important that the GDI is used in combination with other stability indices and dynamical fields, to assess the potential for convection. Validation results suggest that the areas of strongest convection in extra tropical locations such as northern Argentina/Uruguay/Paraguay/southern Brazil or the eastern United States often occur downwind from GDI maxima, and between the GDI maxima and the region of the strongest dynamical forcing. This tendency has been repeatedly confirmed at the WPC International Desks during the routine generation of QPF for North and South America since 2014.

c. Generation of GDI value-convective regime tables

Tables that relate GDI values with expected convective regimes can be established via scatterplots. An example is provided in Figure 9, which presents OLR-GDI scatterplots for two contrasting locations in South America. The large correlations and associated clustering in Minas Gerais, eastern Brazil (right) result on higher confidence GDI-Convective Regime tables. For example, GDI values of 30-40 often associate with OLR values of 160-200 Wm^{-2}. GDI values under 20 rarely associate with OLR values under 230 Wm^{-2}.

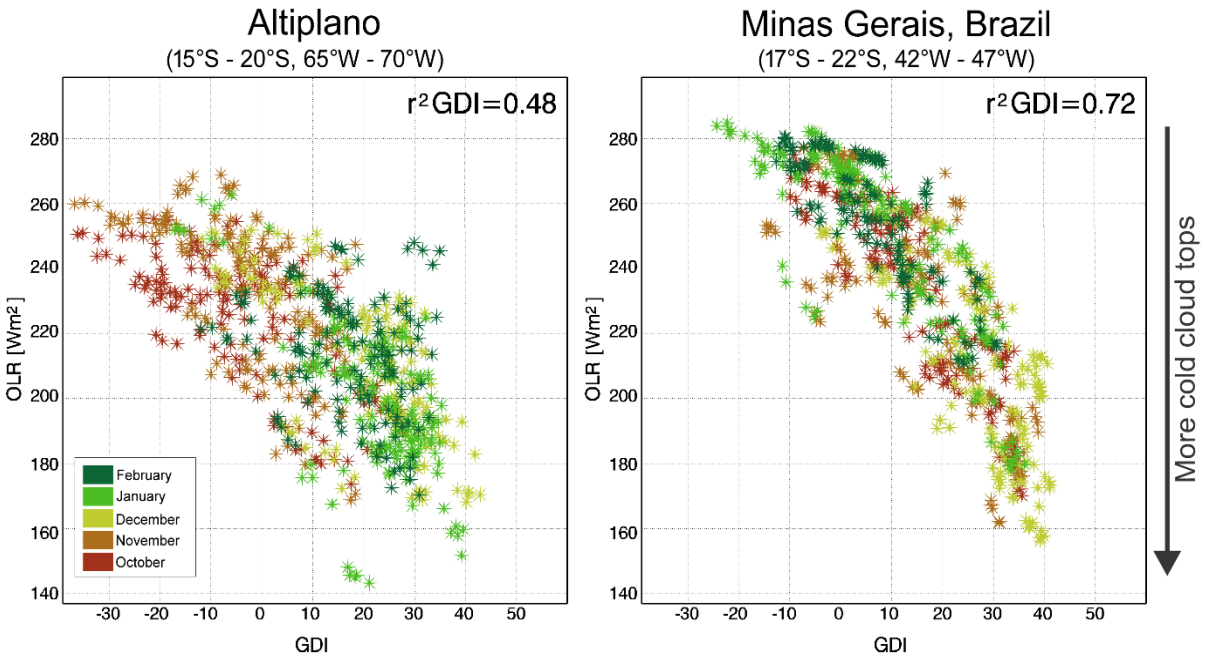

FIG. 9. OLR-GDI scatterplots for two different regions in South America: The Altiplano in the Central Andes (left) and Minas Gerais in southeastern Brazil (right). Colors indicate month, ranging from October 2013 through February 2014, to highlight seasonal changes.

The different distributions in Figure 9 show that the GDI-convection relationship is sensitive to location and seasonality. Correlations over the Altiplano (left), although lower, exhibit strong seasonal variations as suggested by the color coding. Here, dry season convection, shown in browns for October-November, produced a wide scatter. This suggests limited GDI skill during this period. A more linear distribution of greens (January-February) suggests a significant increase on the skill during the wet season, partly tied the seasonal increase in column moisture content.

A more general GDI-convective regime table is presented in Table 4. Although location and seasonality adjustments are suggested, the values presented in Table 4 generally apply to the tropical Americas, especially trade wind regime climates. Values over +20 generally suggest a potential for thunderstorms. This largely increases when values exceed +40. Values under +10 generally suggest the presence of strong inversions and limited thunderstorm potential.

TABLE 4. General GDI-Convection regime table, constructed upon validation results.

GDI Value	Expected Convective Regime
> +45	Scattered to widespread thunderstorms. Locally heavy rainfall likely.
+35 to +45	Scattered thunderstorms and scattered to widespread rain showers. Locally heavy rains possible.
+25 to +35	Isolated to scattered thunderstorms and/or scattered showers. Locally heavy rains possible.
+15 to +25	Isolated thunderstorms and/or isolated to scattered showers.
+05 to +15	Isolated to scattered showers. Any thunderstorm will be brief and isolated.
<+05	Strong trade wind inversion likely. Activity limited to light rain showers.

5. Applicability.

The GDI is applicable for professional fields that require predictions of thunderstorms and other types of convection, with emphasis in the tropical convection and air mass thunderstorms. Many national meteorological centers in the Americas and across the Caribbean have used the GDI for the prediction of convection, and for the generation of quantitative precipitation forecasts since 2014. Some use the GFS-derived index input made available on the WPC International Desks website (http://www.wpc.ncep.noaa.gov/international/gdi/), while others have opted to calculate it in situ. This is the case of the Uruguay Weather Service, the Instituto Uruguayo de Meteorología, where the GDI is calculated from 10km resolution WRF output and is available online at http://www.meteorologia.com.uy/modelos/prediccionNumerica. This is also the case of El Salvador's Ministerio del Medio Ambiente y Recursos Naturales where the GDI is computed routinely from 30km, 15km and 5km WRF model output and is available at http://modelacionnumerica.tk/. Countries that use the GDI routinely in weather forecasting practices include the United States, Chile, Colombia, Costa Rica, Cuba, the Dominican Republic, El Salvador, Honduras, Mexico, Peru, Suriname, Trinidad and Tobago, Uruguay, Venezuela and South Korea (personal communication, 2015 and 2016).

The GDI is also being used as a support tool for civil aviation, where it has proved useful on the planning and adjustment of flight routes. Since 2014, the GDI has been heavily used in support of aviation operations by the Federal Aviation Administration - Air Traffic Control System Command Center in Warrenton, Virginia (Mike Eckert and Joe Carr, FAA, personal communication, 2014); and in 2015 this extended into CWSU Met at ZJX (Jacksonville, FL) with successful results and comments on how the GDI excels particularly under rich westerly flow (Mike Eckert and Joe Carr, FAA, personal communication, 2015). This is when air masses arrive from the Gulf of Mexico, where index skill is enhanced.

The GDI also aids with the detection of waves in the easterly trades and the location of the ITCZ. This skill arises from its ability to capture finer structures that other indices struggle to resolve. This quality makes the GDI particularly useful in Central America, the Caribbean, Mexico and the southeastern United States, where waves in the trades play an important role

in the generation of summer convection and rainfall. An example is provided in Figure 10, which shows the evolution of the GDI and 700-850 hPa streamlines over a three-day period using GFS forecast data. Figure 10 shows the west-northwestward progression of four waves in the trades and associated regions of convective instability. The vorticity at 500 hPa is also included to identify TUTT, a recurrent feature during the Caribbean rainy season. The GDI captures well the instability associated with the cold core of the TUTT by the consideration of mid-level temperatures. In Figure 10, an L is used to denote a TUTT low that meanders from just east of the Central Bahamas into southeastern Florida from July 7th to the 9th while interacting with a wave in the trades. The sequence illustrates how the GDI aids with the detection of trade wind waves A, B, C and D.

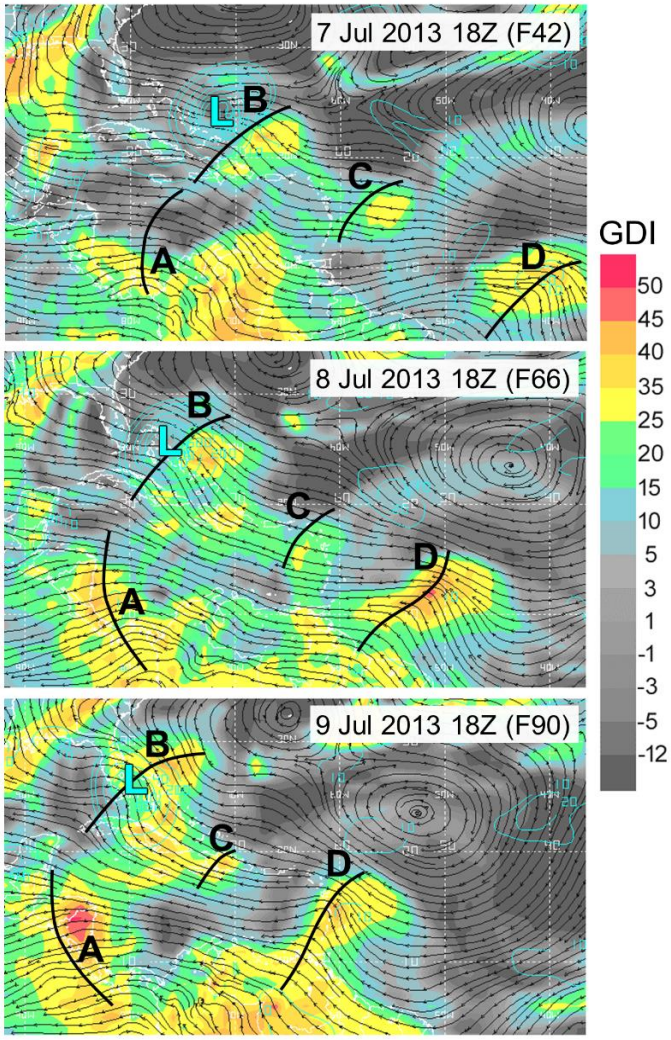

FIG. 10. Three-day sequence of the GDI (shaded), 700-850 hPa streamlines (black) and 500 hPa vorticity × $10^{-6}s^{-1}$ (light blue contours) in GFS model forecast data F42, F66, F90. The sequence shows west-northwestward progression of four waves in the trades: A, B, C and D. TUTT low is indicated with an L.

The GDI loses applicability in latitudes higher than 40°-45° due to the limited amount of heat and moisture in the low and mid troposphere. This is also true for mid latitudes during their cold season, and in cold current environments. Exceptions include robust atmospheric rivers that connect tropical oceans with mid-latitude western coasts. This applies to some of

the cool season rainfall events characteristic of central and southern Chile, and to the west coast of North America. The ability of the GDI to capture such is encouraging for the forecasting of cool season precipitation in mid-latitude western coasts.

Another situation in which the GDI also struggles is near the ITCZ and during rainy season peaks in the deep tropics. This is due to limited variability of mid-tropospheric temperatures and TWI. An additional GDI limitation identified is the overestimation of the potential for thunderstorms in thermal low environments. This is due to the overwhelming contribution of temperature to the calculation of EPT.

6. Concluding remarks and recommendations.

The Gálvez-Davison Index GDI was developed to improve the forecasting of tropical convection, motivated by the limited skill of the traditional stability indices in the tropics. It consists of the algebraic sum of three dimensionless sub-indices. These emphasize processes that dominate the variability of trade wind convection such as the availability of heat and moisture; the stabilizing effects of warm mid-level ridges; and the stabilizing and drying effects of trade wind inversions.

An intercomparison exercise over the Tropical Americas shows that the GDI often relates better to the distribution of cold clouds than the CAPE and the Total Totals, Lifted and the K indices. When using a 2° resolution grid for intercomparison, the GDI outperforms the K in more than 90% of the domain, which stretches from the southern United States to central Argentina and central Chile. It particularly excels in 15°-25° latitude belts, especially over oceans and eastern fringes of continents, where trade wind climates prevail. In these regions, the GDI relates to an additional 15-30% of the cold cloud variance with respect to the K index. Areas of enhanced skill include densely populated locations such as Mexico City, Sao Paulo and Rio de Janeiro. The results suggest that, in these locations, the GDI is the most skillful index for the forecasting of thunderstorms.

The GDI is sensitive to location and seasonality, which requires adjustments to the interpretation of its values. It is also recommended that the GDI be used in combination with other stability indices and dynamical fields to maximize the accuracy when generating a forecast of convection.

Experimental versions of the GDI have already been implemented in several weather services across the Americas, including the US National Weather Service; and is being used routinely for the prediction of thunderstorms, with applications for precipitation forecasting and aviation.

Future work considers more thorough validation exercises using lag correlations and skill scores. Validation exercises should also be extended over longer periods to increase statistical significance. Future work should include the determination of skill tables tailored for specific locations, and optional adjustments that adapt the GDI to locations where its skill is limited.

References

Atkinson, G. D., 1971: Forecasters' Guide to tropical meteorology. TR 240, Air Weather Service, United States Air Force, 388pp.

Betts, A. K., and F. J. Dugan, 1973: Empirical formula for saturation pseudo-adiabats and saturation equivalent potential temperature. *J. Appl. Meteor.*, **12**, 731–732.

Bolton, D, 1980: The computation of equivalent potential temperature. *Mon. Wea. Rev.*, **108**, 1046-1053.

Bryan, G. H., 2008: On the computation of pseudoadiabatic entropy and equivalent potential temperature. *Mon. Wea. Rev.*, **136**, 5239-5245.

Caesar, K. L. 2005: Summary of the Weather during the RICO project. NCAR/Caribbean Institute for Meteorology and Hydrology, 30pp.

Davies-Jones R., 2009: On formulas for equivalent potential temperature. *Mon. Wea. Rev.*, **137**, 3137-3148.

Galway, J. G., 1956: The lifted index as a predictor for latent instability. *Bull. Amer. Meteor. Soc.*, 528-529.

George, J. J., 1960: Weather Forecasting for Aeronautics, Academic Press, 673 pp.

Glickman, T. S., 2000: Glossary of Meteorology. Second Edition. American Meteorological Society, Boston, MA, 855pp.

Grabowski, W. W. and M.W. Moncrieff, 2004: Moisture-convection feedback in the tropics. *Quart. J. Roy. Meteorol. Soc.*, **130**, 3081–3104.

Haklander A. J., and A. Van Delden, 2003: Thunderstorm predictors and their forecast skill for the Netherlands. *Atmospheric Research*, **67-78**, 273-299.

Holton, J.R., 1972. An Introduction to Dynamical Meteorology. Academic Press, 319 pp.

Huntrieser, H., Schiesser, H.H., Schmid, W., Waldvogel, A., 1997. Comparison of traditional and newly developed thunderstorm indices for Switzerland. *Weather Forecast.*, **12**, 108–125.

Jacovides, C.P., Yonetani, T., 1990. An evaluation of stability indices for thunderstorm prediction in Greater Cyprus. *Weather Forecast.*, **5**, 559–569.

Liebmann B. and C.A. Smith, 1996: Description of a Complete (Interpolated) Outgoing Longwave Radiation Dataset. *Bull. Amer. Meteor. Soc.*, **77**, 1275-1277.

Miller, R. C., 1967: Notes on analysis and severe storm forecasting procedures of the Military Weather Warning Center. Tech. Rept. 200(R), Headquarters, Air Weather Service, USAF, 94 pp.

Miller, R. C., 1972: Notes on analysis and severe storm forecasting procedures of the Air Force Global Weather Central. Tech. Rept. 200(R), Headquarters, Air Weather Service, USAF, 102 pp.

Neelin, J. D. and I. M. Held, 1987: Modeling tropical convergence based on the moist static energy budget. *Mon. Weather Rev.*, **115**, 3–12.

Peppler, R.A., Lamb, P.J., 1989: Tropospheric static stability and central North American growing season rainfall. *Mon. Weather Rev.*, **117**, 1156–1180.

Ramage, 1995: Forecasters Guide to Tropical Meteorology. Updated. Tech. Rept. Air Weather Service Scott AFB IL, 492 pp.

Randall D. A. and G. J. Huffman, 1980: A stochastic model of cumulus clumping. *Journal of the Atmospheric Sciences*, **37**, pp. 2068-2078.

Raymond D. J., 2000a: Thermodynamic control of tropical rainfall. *Q. J. R. Meteorol. Soc.*, 126, pp. 889-898.

Raymond D. J., 2000b: The Hadley Circulation as a Radiative-Convective Instability. *J. Atmos. Sci.*, **57**, 1286-1297.

Riehl, H., 1954: Tropical Meteorology. McGraw-Hill, New York-London, 1954. 392 pp.

Sadler, J. C., 1967: The tropical upper tropospheric trough as a secondary source of typhoons and a primary source of trade wind disturbances. Hawaii Institute of Geophysics, University of Hawaii, HIG 67-12 and AFCRL 67-0203, 44pp.

Schultz, P., 1989. Relationships of several stability indices to convective weather events in northeast Colorado. *Weather Forecast*. **4**, 73–80.

Showalter A. K., 1947: A stability index for forecasting thunderstorms. *Bull. Amer. Meteor. Soc.*, **34**, 250-252.

Tompkins, A. M., 2001: Organization of Tropical Convection in Low Vertical Wind Shears: The Role of Cold Pools. *J. Atmos. Sci.*, **58**, 1650–1672**.**